



Cite this: *Analyst*, 2025, **150**, 4414

A low-cost point-of-care device for the simultaneous detection of two sexually transmitted bacterial pathogens in vaginal swab samples

Erin K. Heiniger, *† Kevin P. Jiang, † Sujatha Kumar and Paul Yager

Curable sexually transmitted infections (STIs) caused by the bacteria *Chlamydia trachomatis* (CT) and *Neisseria gonorrhoeae* (NG) are widespread globally. These infections are particularly dangerous for female patients, causing pelvic inflammatory disease, infertility, and increased risk of HIV acquisition. Vaginal self-swab sampling can improve access to STI screening but is still subject to treatment delays due to centralized processing. A low-cost point-of-care (POC) device capable of detecting these bacteria from a self- or clinician-collected vaginal swab could address this delay and allow for more timely treatment. In this work, vaginal swab materials from patients infected with CT or NG required a filtration step before lysis and loop-mediated isothermal amplification (LAMP) detection using a UbiNAAT device. We have shown a simple, low-cost sample preparation method that supports rapid DNA detection from NG and CT on our POC UbiNAAT platform.

Received 6th May 2025,

Accepted 7th August 2025

DOI: 10.1039/d5an00496a

rsc.li/analyst

Introduction

There are over 1 million new curable sexually transmitted infections (STIs) globally every day.¹ The most common bacterial STIs are caused by *Chlamydia trachomatis* (CT), *Neisseria gonorrhoeae* (NG), and *Treponema pallidum* (TP), in decreasing prevalence; together these bacteria accounted for 2.5 million new infections in the United States in 2022.² Despite a large portion of CT and NG infections being asymptomatic, they can still cause adverse outcomes, especially in female patients, including pelvic inflammatory disease, infertility, and increased risk of HIV acquisition.^{3,4} Worryingly, strains of NG that are antimicrobial resistant (AMR) or even multi-drug resistant (MDR) have increased in prevalence recently,⁵ prompting changes in treatment guidelines. Since 2020, the recommended treatment for uncomplicated NG has been administration of a single antimicrobial agent, ceftriaxone.⁶ When NG strains resistant to ceftriaxone emerge, clinicians may run out of suitable treatment options.

One of the key strategies suggested by the World Health Organization (WHO) for controlling STIs is increased access to screening.¹ Barriers to widespread screening for STIs include social stigma, worries about confidentiality, and cost.⁷

Currently, NG and CT are diagnosed mainly by nucleic acid amplification testing (NAAT, e.g. polymerase chain reaction (PCR)); while culture or gram staining can be used, NAATs are considered more accurate, especially for asymptomatic infections.⁸ For female patients, urine samples have been widely used for diagnosis, and intriguing devices have been developed for the use of urine at the point of care.⁹ However, as a sample, urine suffers from sensitivity variations (clean-catch *versus* first-catch sampling protocols) and low pathogen concentrations. A recent meta-analysis of vaginal swab samples shows them to be more sensitive than urine samples.¹⁰ One way to lower screening barriers is to implement self-collection of the clinical sample. Several studies have demonstrated the feasibility of using self-collected vaginal swab samples for the diagnosis of CT and NG.^{11–14} Any differences in sample self-collection *versus* clinician-collected samples have been outweighed by the benefits of increased screening, including better reach toward first-time testers.¹³ Female patients and their children suffer increased negative sequelae as a result of CT or NG infection,¹⁵ compared to other patient populations.

However, self-sampling alone cannot guarantee better patient outcomes. Part of the problem is the time it takes to receive a result: up to 9 days in a typical healthcare system.¹⁶ The on-site use of the Cepheid GeneXpert rapid quantitative polymerase chain reaction (qPCR) CT/NG test instead of processing in an off-site hospital laboratory reduced the time from testing to treatment from 7–14 days to 2 days.¹⁷ A 30-minute point-of-care (POC) test for CT/NG (Binx Health *io*)

Department of Bioengineering, University of Washington, Seattle, WA 98105, USA.
 E-mail: erinkh@uw.edu

†These authors contributed equally to this work.



was shown to reduce time to treatment, as well as reduce unnecessary antibiotic treatment through improved specificity, but also increased the cost of testing.¹⁸ The Visby Medical PCR point-of-care disposable diagnostic device was shown to be sensitive and specific for CT, NG, and *Trichomonas vaginalis* (TV).¹⁹ Though the Visby device is an exciting development in the field, and it has just been approved by the FDA for over-the-counter sale in the USA, it is complex and expensive, especially for a single-use test (approximately \$75 per multiplexed test when purchased in bulk).²⁰ While it tackles the issue of long wait times between the sample and the result, its cost could hamper its effectiveness in low-resource settings. While the Visby home STI testing device already on the market demonstrates the applicability of this type of testing outside of the clinic, we believe that there is still room for different approaches like the UbiNAAT device that could be less expensive. Non-NAAT rapid diagnostic devices are less expensive but have been shown to lack the sensitivity and specificity required for impactful screening and treatment of patients.^{16,21} Therefore, the diagnostic device with the most impact would (1) analyse self-collected vaginal swab samples, (2) be a sensitive and specific NAAT, (3) be widely available and inexpensive, (4) be easy to use, and (5) provide results in 30–60 minutes, ideally before a patient leaves the clinic. It is conceivable that these technologies could also be used in the home due to their speed and avoidance of social stigma, but home testing may have public health logistics that need to be addressed before its widespread use.²²

Increasingly, isothermal amplification NAATs have been investigated for their use in low-resource settings; their need for only a single incubation temperature (as opposed to the temperature cycling protocol of PCR) reduces the complexity of running these assays. One of the most commonly used isothermal methods is loop-mediated isothermal amplification (LAMP); it uses 4 to 6 primers, 2 of which create looped products that allow exponential amplification by a strand displacing polymerase.^{23,24} This method is fast, sensitive, has greater resistance to inhibitors than PCR,²⁵ and can be coupled to reverse transcriptase (RT) activity for detecting RNA.^{26,27} During the SARS-CoV-2 pandemic, LAMP technology advanced rapidly since the speed and technical ease of using the assay were particularly attractive for product development.^{28,29} LAMP has been incorporated into microfluidic devices, allowing for the future detection of pathogens outside the laboratory.³⁰

In this work, we demonstrate the detection of CT and NG DNA from clinical vaginal swab samples in a prototype of an inexpensive point-of-care integrated device based on our previous work demonstrating a swab-to-result respiratory panel diagnosis on a low-cost (~\$3 in single-use disposable parts/reagents) UbiNAAT platform (Fig. 1A).³¹ Briefly, a patient swab is inserted into the device and agitated in a nuclease-inactivating lysis buffer stored on the device. Then, the device is activated and automatically heats the sample to lyse the cells and release the nucleic acids. Lysate is allowed to flow into porous membranes carrying lyophilized LAMP reagents. The amplification regions are heated via a printed circuit board and fluo-

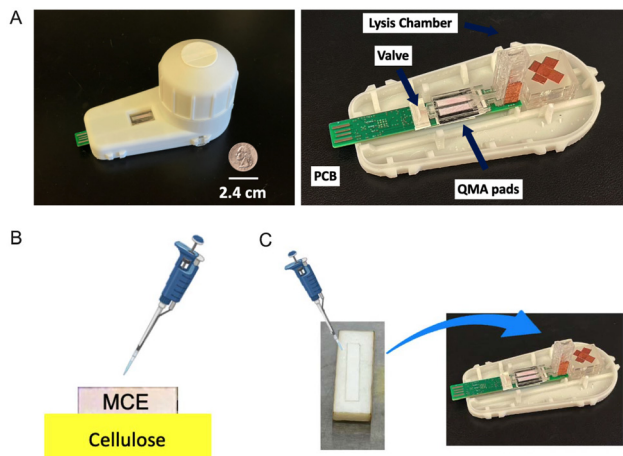


Fig. 1 A UbiNAAT integrated device. (A) Fully assembled device (left) and device without top enclosure (right). (B) A mixed cellulose ester (MCE) filtration setup with a cellulose wicking membrane. (C) Transfer of the MCE membrane post-filtration and rinsing into the lysis chamber of the UbiNAAT device. Images in (B) and (C) are not to scale.

rescence signal amplification is detected *via* cell-phone imaging. Here, the UbiNAAT device was successfully adapted to detect CT and NG DNA from clinical vaginal swabs after filtration. Because of its ease of use, this technology will also be appropriate for the diagnosis of STIs in a home setting, with results transmitted to clinicians for treatment decisions through the same cell phone that is used to read the test results.

Experimental

NG and CT cultivation and use

NG cells were purchased from ATCC (19424) and stored frozen at -80°C in 25% glycerol. Before use in experiments, the frozen material was streaked on a Chocolate Agar II plate (#221267; BD Diagnostics, Franklin Lakes, NJ, USA) and incubated at 37°C in a high- CO_2 bag (GasPak EZ CO_2 Pouch, #260684; BD Diagnostics) for 48 hours. Then, a single colony was picked and spread on a new Chocolate Agar plate, and incubated as above for 24–48 hours. After incubation, the cells were scraped from the surface of the plate and resuspended in 10 mM Tris and 0.1 mM EDTA (ethylenediaminetetraacetic acid) buffer (TE). Absorbance at 600 nm was measured and compared to a standard curve of known cell concentrations to estimate the cell concentration (SpectraMax iD3, Molecular Devices, San Jose, CA, USA). The cells were diluted in TE to the desired concentration.

CT-infected epithelial cells were gifted to us by collaborators, who estimated the cell concentration by microscopy and delivered cells to us on ice. After receipt, the infected cells were frozen in small aliquots and stored at -80°C . Before use, the cells were thawed and gently mixed.

PCR quantification of bacterial DNA

Genomic copy numbers of bacterial pathogens in clinical samples were determined using conventional quantitative PCR. Sequences of the PCR primers and probes used are found in Table S1. For quantifying the NG chromosome, we used primers and probe from Hjelmevoll *et al.* (2006),³² adapted for use with a SensiFAST Probe No-ROX kit (BIO-86050; Meridian Bioscience, Memphis, TN, USA). The qPCR reaction included a 1× kit master mix, 400 nM each primer, 100 nM probe, and 1–5 µL of template per 20 µL reaction. Reactions were run on either of the two qPCR thermocyclers, a CFX-96 Touch or a CFX Opus (Bio-Rad, Hercules, CA, USA). Purified, quantified NG genomic DNA (#19424DQ; ATCC, Manassas, VA, USA) was used to build a standard curve. DNA from clinical samples was purified (DNeasy blood and tissue kit, Qiagen, Hilden, Germany) before qPCR determination of copy number. The NG DNA starting concentration was calculated *versus* the standard curve using CFX Manager software (Bio-Rad), which employs a multivariable, nonlinear regression model to calculate an amplification threshold.

Testing with swabs is not inherently quantitative, due to swab-to-swab sampling errors. However, it was incumbent on us to determine how sensitive our device is for diagnosis from swabs. Two different qPCR assays were used to quantify CT plasmid DNA. CT assay 1 (Table S1), modified from Dhawan *et al.* (2014),³³ was performed as above, using a SensiFAST Probe kit. Our laboratory lacks the capability to grow tissue culture cells and propagate CT bacteria on them. We were gifted a limited quantity of CT-infected epithelial cells for use in this project. Due to this limited availability of CT cells, we were unable to purify the cryptic plasmid in high enough numbers to build a standard curve for quantification. The standard curve was initially built using purchased quantified DNA (VR-348BD; ATCC), which contained a mixture of chlamydia and human DNA. Because this source of DNA was mixed at an unknown ratio, we could not report CT concentration accurately in terms of CT plasmid copy number using this standard curve. To rectify this uncertainty, we engineered a plasmid sequence to serve as a second known standard (see SI Methods for plasmid construction details). Quantified plasmid was compared to mixed CT and human genomic DNA using a SensiFAST SYBR qPCR kit (Meridian Bioscience). Forward and reverse primers from CT assay 2 were used at 400 nM each. We found an average of 3 cryptic plasmid copies per femtogram of mixed DNA standard. Using this value, we converted our measured fg DNA equivalents to plasmid copies for all CT concentrations. DNA from clinical samples was purified (DNeasy kit, Qiagen) before qPCR determination of copy number.

LAMP assay

The LAMP assay reagents consist of a WarmStart LAMP kit (New England Biolabs (NEB), Ipswich, MA, USA), an SYTO-82 fluorescent intercalating dye (Thermo Fisher Scientific, Waltham, MA, USA), hydroxynaphthol blue (HNB) (Millipore Sigma, Burlington, WA), trehalose (Life Sciences Advanced

Technologies), dextran 500 kDa (Sigma-Aldrich, St Louis, MO, USA), nuclease-free water (Thermo Fisher Scientific), and assay-specific LAMP primers (Integrated DNA Technologies (IDT), Coralville, IA, USA). Primer sequences are shown in Table S2. The final concentrations of all components can be found in Table S3.

LAMP mixes were prepared at 20 µL volumes inside PCR reaction tubes, homogenized on a vortex mixer, and heated using a BioRAD Real-Time thermocycler (CFX Opus) at 63 °C for 60 minutes. Signal liftoff times were determined using CFX Maestro software to set the amplification threshold as described above.

Commercial swab spiking and lysis

Purchased vaginal swabs from healthy volunteers (991-25-S-3; Lee Biosolutions, Maryland Heights, MO, USA) that were negative for both target pathogens were shipped frozen and dry (without buffer). BD BBL CultureSwab Sterile, Media-free Swabs (BD Diagnostics) are used for this product. Lysis buffer was based on the HUDSON (“heating unextracted diagnostic samples to obliterate nucleases”) solution protocol.³⁴ Briefly, 2.5 mM Tris(2-carboxyethyl)phosphine hydrochloride (TCEP) (Millipore Sigma), 10 mM Tris-HCl pH 8.0 (Invitrogen by Life Technologies), and 1 mM ethylenediaminetetraacetic acid (EDTA) (Invitrogen by Life Technologies) are combined and used with heating (95 °C for 5 minutes) to inactivate nucleases and other interfering proteins in the vaginal swab matrix.³⁵

On the day of use, each swab was equilibrated to room temperature, then submerged in 460 µL of lysis buffer. The swab was agitated by twirling for 10 seconds before removal, during which time buffer was squeezed from the swab by pressing it against the side of the tube. For each tested sample, 114 µL of swab material dissolved in lysis buffer was mixed with 6 µL of NG cells or CT-infected epithelial cells for a 120 µL sample. Spiked samples were heated to 95 °C for 5 minutes in a heat block (Digital dry block heater, VWR, Radnor, PA, USA). After heating, the samples were allowed to cool to room temperature. Then, a portion was used to rehydrate lyophilized LAMP reagents. The remaining sample was used as a template for qPCR to quantify the NG or CT DNA content.

Clinical swab source

As a benefit of our funding mechanism, we received vaginal swab exudates from self-collected vaginal swabs (Copan FLOQ swabs) that had been sent dry to clinical collaborators at the Point-of-care Technology Research Network (POCTRN) center at Johns Hopkins University (JHU). A portion of each swab exudate was analyzed using a Hologic STI system at JHU and determined to be positive or negative for both NG and CT. The remaining exudate (expressed in TE buffer (10 mM Tris, 1 mM EDTA)) was frozen and then shipped to the University of Washington on dry ice. Samples were stored at –80 °C until use, when they were thawed and gently mixed before use.



Mixed cellulose ester (MCE) filtration

Mixed cellulose ester filters with an average pore size of 0.22 μm (0.22 μm MCE membrane, Merck Millipore) were cut into 3 mm \times 15 mm pieces using a high-powered CO₂ laser cutter (VLS3.60 CO₂ laser, Universal Laser Systems, Scottsdale, AZ, USA). Each filter was placed on a 22 mm \times 16 mm \times 2.5 mm cellulose wicking pad (Fig. 1B). Then, 200 μL of

expressed clinical vaginal swab sample was pipetted onto the MCE and allowed to wick through. Next, 200 μL of TE (10 mM Tris and 0.1 mM EDTA) was pipetted onto the upper surface of the filter. After allowing five minutes for fluid to flow through the membrane, the MCE filter was removed from the cellulose using forceps, and then placed in a 1.5 mL microfuge tube (#3451, Thermo Fisher Scientific, Waltham, MA, USA) and covered with 200 μL of TE/HUDSON buffer. Alternatively, the

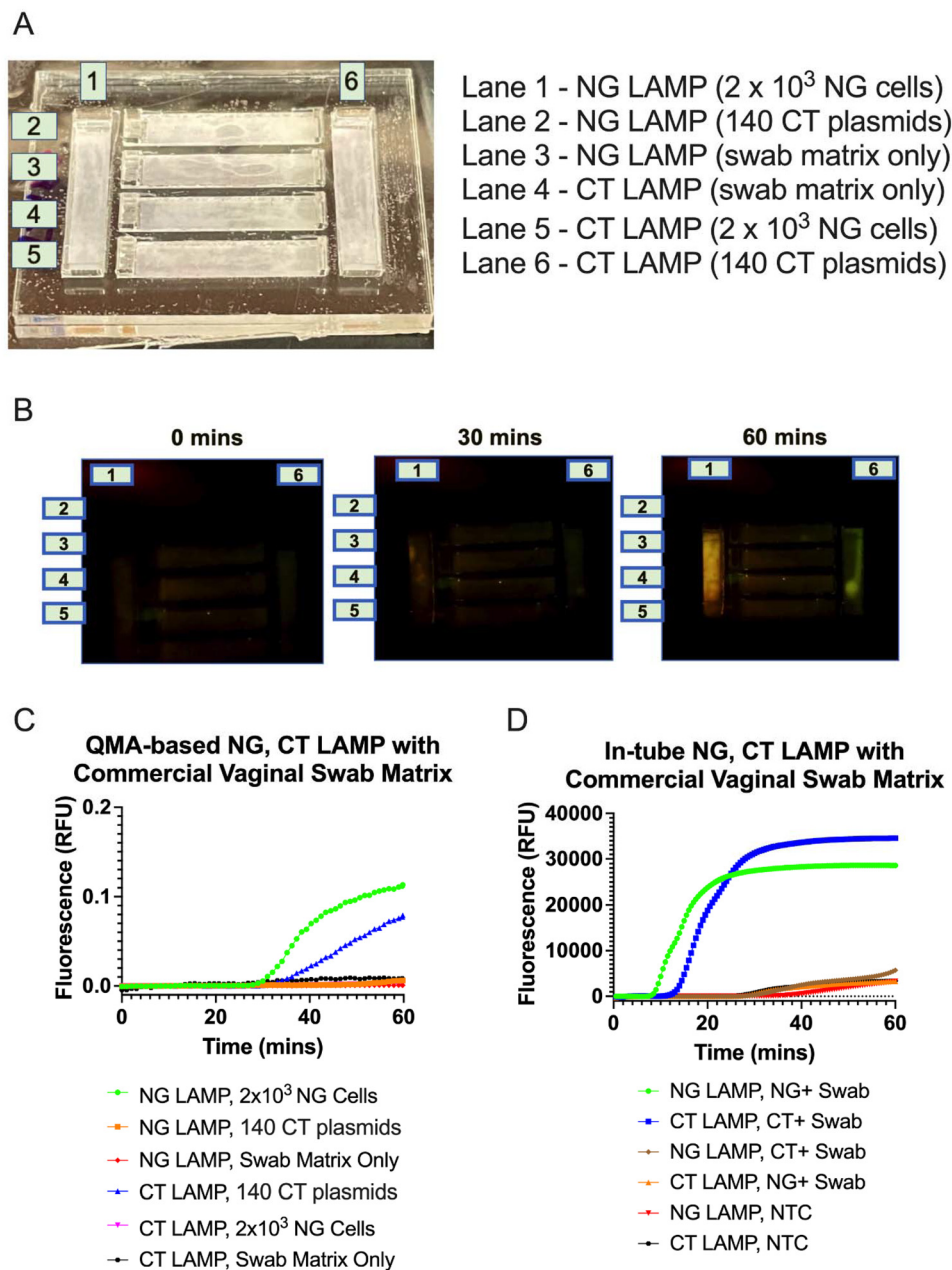


Fig. 2 Six-pad test device running lyophilized LAMP on a QMA membrane with commercial vaginal swab lysate spiked with *Neisseria gonorrhoeae* (NG) or *Chlamydia trachomatis* (CT) bacterial cells. (A) Six-pad PMMA tray holding 6 QMA membranes with rehydrated NG or CT LAMP reagents. (B) Representative images of fluorescence for signal amplification in-paper as imaged using a cell-phone reader showing fluorescence signal growth across 60 minutes. (C) Quantified NG and CT LAMP results from QMA membrane image stacks. The results are representative of reproduced replicates. (D) In-tube NG and CT LAMP processed using a BioRAD CFX thermocycler with commercial vaginal swab lysate spiked with *Neisseria gonorrhoeae* (NG) or *Chlamydia trachomatis* (averaged fluorescence signal across $n = 3$ replicates) (see Fig. S4 for all reaction curves).



filter was placed directly into the UbiNAAT device (described below). CT or NG DNA was released into the buffer phase by heating to 95 °C for 5 minutes.

Amplification pad test devices

The assembly of devices and the preparation of porous membranes for testing porous matrix-based reactions was previously described in Jiang *et al.* (2024).³¹ Briefly, transparent devices were built that enclosed six identical porous pads ("six-pad devices"). The six pads were oriented to be visualized within the field of view of the cell-phone fluorescence reader (see Fig. 2A). Each LAMP reaction was performed in an individual Whatman quartz fiber membrane (QMA) from Cytiva (VWR, Radnor, PA, USA) that had been pre-loaded with LAMP reagents and dried. The pads were placed inside a 33 mm × 26 mm × 1/16 inch polymethyl methacrylate (PMMA) device (McMaster-Carr, Elmhurst, IL, USA). The bottom PMMA shell held six channels (16.7 mm × 3.3 mm) that were laser-etched to a channel depth of 600 µm, while the top shell placed vents at both ends of each channel to allow for fluid addition and air venting. After insertion of the QMA pads, the top and bottom enclosures of the six-pad devices were bonded together using polydimethylsiloxane (PDMS) pressure-sensitive tape (Valley Industrial Products, Huntington, NY, USA). All porous materials, PMMA pieces, and films were machined and etched on the aforementioned CO₂ laser cutter. For each QMA reaction pad, the pad was filled with 25 µL of template solution, the PMMA top enclosure vents were sealed using a Microseal B adhesive sealer (BioRad), and the sealed device was placed in a custom-made, dual-sided (ITO glass top) heater oven at 64 °C for 60 minutes to support the LAMP reaction.

Lyophilization in tubes and pads

LAMP reagent lyophilization protocols were followed as described in our previous studies.^{31,36} In short, QMA fiber pads that had been blocked in 1% BSA (GeminiBio, Sacramento, CA, USA) and 0.1% Tween 20 (Sigma-Aldrich, St Louis, MO) were held in a 6-well plate and hydrated with 24 µL of LAMP reaction mixture (no template) (see Table S3). The plate was quickly flash-frozen in liquid nitrogen before being connected to a FreeZone 2.5 liter freeze-drying benchtop lyophilizer (Labconco, Kansas City, MO, USA) through a fast-freeze flask (Labconco) and vacuum-dried overnight.

UbiNAAT device fabrication

The 2-plex UbiNAAT device (Fig. 1A) assembly protocol and fabrication of the device components (a microfluidic internal device, a 3D printed enclosure, and a custom printed circuit board) were described previously.^{31,37–40} In this study, the device was modified by removing the blister containing sample lysis solution and the blister fluidic path was covered with copper tape. At the start of a sample process run, the post-capture MCE membrane was inserted into the lysis chamber using tweezers and pushed to the bottom of the lysis chamber (see Fig. 1). 200 µL of HUDSON inactivation solution

was pipetted through the top of the lysis chamber to ensure full submersion of the MCE membrane.

Fluorescence detection with a cell phone

QMA pad-based LAMP reactions were visualized *via* a cell-phone-based fluorescence reader as described in Jiang *et al.* (2024).³¹ The reader consisted of a Google Nexus 5X with two interference filters: an FES0550 emission short-pass filter (Thorlabs, Newton, NJ, USA) placed over the phone's camera lens and a BP 587/25 excitation filter (Zeiss, Oberkochen, Germany) placed over the phone's light-emitting diode (LED). The filters were held in a custom black PMMA fixture, with a 12 mm wide, 12 mm focal length plano-convex lens (Edmund Optics, Barrington, NJ, USA) placed 6 mm from the phone's LED (before the excitation filter).³¹ The cell-phone reader was fixed at 8.5 cm above the amplification device, with images taken at 60 second intervals using the phone's incandescent white balance, 1/5 aperture, 200 ISO, and manual focus settings. Image stacks from each 60 minute run were transferred to a desktop computer *via* a USB connection.

As previously described by Shah *et al.* (2022), a custom MATLAB script was used for fluorescence image analysis.³⁷ Similar to the analysis method in Jiang *et al.*, the top 1% of pixel intensity within a selected region-of-interest (ROI) for each pad was used to determine fluorescence intensity changes across each minute to generate a fluorescence amplification curve over time.^{31,37,38} Background subtraction was performed by subtracting the average fluorescence intensity from 5–10 minutes from each image, and a 0.02 RFU fluorescence threshold was used to determine the amplification liftoff time for distinguishing positive and negative clinical samples in each LAMP reaction.^{31,37}

UbiNAAT diagnosis from clinical samples

As previously demonstrated in Jiang *et al.*, the UbiNAAT detection device can incorporate lysis, fluidic movement, and simultaneous amplification detection for at least two assays (two in its current configuration).³¹ Here, we utilized the same platform to assess vaginal swab clinical samples for *Neisseria gonorrhoeae* (NG) and *Chlamydia trachomatis* (CT). The device utilized the PCB heater and PID loop previously developed in the laboratory and described by Shah *et al.* (2023), which was shown to be functionally equivalent to benchtop equipment for performing lysis and amplification heating.^{31,36} Fluidic control was enabled using a terminal "air spring valve", which was activated by resistive heating after completion of the lysis step.³¹ Each 2-plex UbiNAAT device contained two lyophilized QMA LAMP pads, one each for separate NG and CT assays, with amplification heating performed at 63 °C across both pads.

At the start of each run, the vaginal clinical samples were treated using MCE filtration and bacterial capture, which was shown in-tube and on QMA membranes to be necessary to remove amplification inhibitors present in those samples. Following clinical sample flow-through and washing of the MCE filter, the membrane was transferred to the UbiNAAT



lysis chamber *via* tweezers and pushed to the bottom of the chamber. The addition of TE-HUDSON solution *via* pipette was chosen to ensure that the MCE membrane was fully submerged in liquid, as the membrane was not fixed to any part of the lysis chamber and could be pushed against the chamber walls through the introduction of solution from below. PCB lysis heating was then followed at a setting of 100 °C for 7 minutes, followed by 3 minutes of cooling. The terminal air spring valve was then opened to enable flow of the lysed clinical sample through the device to rehydrate both assay pads. Amplification heating began following assay pad rehydration; images of both pads were acquired using a cell-phone fluorescence reader at 60 second intervals for 60 total minutes. Fluorescence images were quantified as described above.

Results and discussion

In the work described in this paper, we found that vaginal swab samples from JHU patients contained amplification inhibitors of LAMP; we also found that these inhibitors could be excluded from the sample by crude filtration. The filter captures the pathogenic bacteria and can be input to the UbiNAAT device for cell lysis followed by LAMP fluorescence detection of pathogen DNA in a POC-compatible manner.

Commercial swabs spiked and treated with HUDSON

For initial evaluation of the proposed diagnostic device, we purchased “normal” (non-disease-state) vaginal swab samples from a commercial source (Lee Biosolutions) and then spiked them with CT or NG bacteria as described above. Spiked samples were then used to rehydrate LAMP reagents previously lyophilized in QMA porous pads and incubated at 63 °C for amplification. Our previous work showed that nasal swab samples could be treated in this manner and supported the amplification of viral RNA with no further sample preparation.³¹ We used here a LAMP assay that targets the *porA* locus on the NG DNA genome, which was shown to be sensitive and highly specific for NG in several studies.^{41,42} We observed amplification from the NG-spiked sample when NG primers were used (Fig. 2A and B). Likewise, the CT-spiked samples amplified when CT primers were used. Cross-reactivity of the LAMP primers was not observed, as NG-spiked samples did not amplify when CT primers were used or *vice versa*. Non-spiked samples did not amplify when either primer set was used, confirming that these samples were negative for both CT and NG before spiking. These results led us to believe that vaginal swab samples could be used on devices with this simple sample preparation method. A simple protocol is ideal for delivering a diagnostic device at the lowest possible cost.

In the QMA pads, we observed amplification liftoff at 30–35 minutes after the start of amplification heating (representative reaction in paper is shown in Fig. 2B and C). When the sample was used to rehydrate LAMP reagents in PCR tubes, we observed liftoff at 10–15 minutes while retaining specificity (Fig. 2D). These results are consistent with our pre-

viously reported observation that amplification in our porous membranes has been slower than in PCR tubes.³¹ We speculate that heating conditions and membrane treatment—perhaps the BSA coating required to prepare the membrane for lyophilization—interfered with the speed of the reaction, but we have no definitive evidence of the latter hypothesis.

Surprisingly, JHU clinical swab samples inhibited amplification

We initially believed clinical swab samples provided by JHU could be processed the same way as those from the commercial source because they used almost identical buffers (10 mM Tris with either 1 mM EDTA (JHU) or 0.1 mM EDTA (commercial)) and similar swabs. For initial testing of the JHU swab material, we took a portion of several samples, added TCEP to a final concentration of 2.5 mM, and used a thermal lysis protocol. However, when these samples were used to rehydrate LAMP reagents lyophilized in the tube, we noted that many of them changed the color of the solution (Fig. 3A). Hydroxynaphthol blue (HNB), which is used in the UbiNAAT device to reduce background fluorescence and improve the signal-to-noise ratio,³¹ is purple in the presence of higher concentrations of divalent cations, such as Mg²⁺ and Ca²⁺, and blue in lower concentrations.^{43,44} When DNA in buffer was

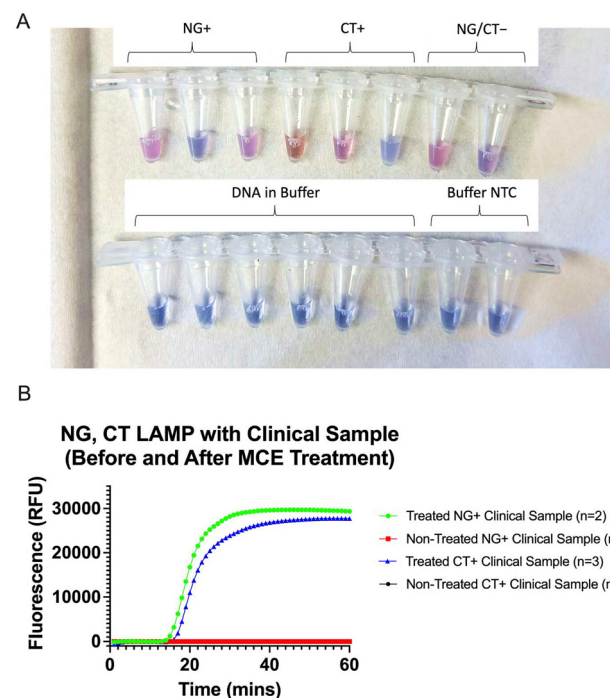


Fig. 3 Filtration of clinical vaginal samples enabled in-tube LAMP reactions. (A) Comparison of lyophilized LAMP reagents rehydrated with clinical vaginal samples (top row) and buffer samples (bottom row). (B) Quantified averaged *Neisseria gonorrhoeae* (NG) ($n = 2$) and *Chlamydia trachomatis* (CT) ($n = 3$) signals. LAMP results for the QMA membrane comparing treated and non-treated clinical vaginal samples (see Fig. S5 for all reaction curves).



used to rehydrate the same reagents, the solution remained blue.

This color change was accompanied by inhibition of LAMP amplification (Fig. 3B). Of the samples tested, there was variable inhibition of amplification, and this inhibition was not limited to swabs from NG- or CT-infected people, as the negative samples were also inhibitory (data not shown). Because HNB is a metal cation indicator, we hypothesized that the inhibitory element was likely an excess of ions in the clinical solutions provided by JHU. LAMP has some tolerance to increased Mg^{2+} concentration, but is inhibited at concentrations above 8 mM in a dose-dependent manner (Fig. S3). The inhibition by the clinical samples was relieved by a 1:4 dilution (Fig. S2), which suggests that the concentration of the unknown factor was reduced to below its inhibitory threshold. While dilution of the sample could be a simple remedy to the issue, it would proportionally reduce the sensitivity of the assay in the UbiNAAT device, nullifying the advantage of using a NAAT rather than an antigen detection diagnostic device.

Inhibition of clinical swab amplification overcome by MCE filtration

To remove soluble inhibition factors like divalent cations, we applied the JHU samples to an MCE membrane (Fig. 1B), which we previously showed to be capable of capturing NG- and CT-infected epithelial cells with high efficiency (manuscript in preparation). We washed the captured cells and then transferred the MCE membrane bearing the cells into lysis buffer (TE/TCEP). After heating to lyse the cells, bacterial DNA was found in the solution by qPCR analysis. When we used this lysate solution to rehydrate LAMP reagents in a PCR tube, pathogen amplification was restored (Fig. 3B), indicating that the inhibitory element had been removed by the filtration and washing processes.

We do not currently understand the ways in which the Lee Bioscience vaginal swab samples differ from those obtained from JHU. As we described above, the Lee Bioscience samples were obtained using BBL culture swabs, which are then frozen and shipped dry. Upon use, the swab material is eluted into the TE/HUDSON lysis buffer (10 mM Tris, 1.1 mM EDTA, 2.5 mM TCEP) by manual agitation/swirling for 10 seconds. The JHU swab material was self-collected at the subject's home using a Copan FLOQ swab, shipped dry to JHU, and then eluted into 10 mM Tris and 1 mM EDTA. Then, they were frozen and shipped to UW Seattle. In previous work, we showed that FLOQ swabs are compatible with LAMP amplification (data not shown), so it is unlikely that they are the source of the filterable amplification inhibitor found in the JHU samples. One possible hypothesis is that the JHU population of women could have had significantly higher Mg^{2+} and/or Ca^{2+} concentrations in vaginal mucus than other populations, perhaps due to factors such as the presence of high-calcium seminal fluid.⁴⁵ It should be noted that all commercial samples from Lee Bio were specifically pre-coital, so should not contain semen. There could also be patient-to-patient variation in Fe^{2+} from heme breakdown, depending on how close

sampling was to menses. It is a limitation of this study that there were not enough patient samples available to test these hypotheses. Any number of factors such as the sample site preparation, sample storage, and/or patient education could also prove impactful to the accuracy of a vaginal swab diagnostic device. We will pursue the answers to these questions in future work.

LAMP assay of MCE-filtered clinical samples in QMA membranes

Six-pad devices were designed to test the compatibility of QMA-based LAMP assays with vaginal swab clinical samples for NG and CT. Each six-pad device held three lyophilized QMA LAMP pads for each of the NG and CT LAMP assays (one positive sample, one negative sample, and one non-specific sample that contained another pathogen).

Prior to filtration of the clinical samples through mixed cellulose ester (MCE) pads, both NG and CT LAMP assays in QMA membranes showed no amplification over the course of an hour; this was true for positive, negative, and non-specific conditions. As seen in Fig. 4A, none of the assay pads showed a fluorescence amplification signal during 60 minutes of heating. Quantified amplification curves, shown in Fig. 4B, indicated no amplification liftoff following background subtraction. The lack of difference between positive, negative, and non-specific assays suggested strong inhibition of LAMP activity by the clinical samples across both assays. Repeated testing with additional clinical samples yielded a similar lack of amplification.

Following mixed cellulose ester (MCE) pad treatment of clinical samples, amplification was restored for both NG and CT LAMP assays in QMA membranes. Both the NG-positive and CT-positive samples showed strong amplification for their respective LAMP assays across the entirety of the assay pads (Fig. 4C). Quantified curves showed early signal detection for both assays, with amplification liftoff achieved by 30 minutes for both NG and CT LAMP (Fig. 4D). Cross-reactivity test samples (samples containing pathogen(s) not targeted by the specific assay) and negative clinical samples across both assays showed no amplification after an hour of heating, with quantified amplification curves remaining flat.

MCE-treated STI clinical samples amplified in a fully assembled 2-plex UbiNAAT device

Fifteen clinical vaginal samples were processed on the UbiNAAT platform (five positive NG samples, five positive CT samples, and five double-negative samples). To determine the bacterial load in each sample run and ensure that reagents were not contaminated, qPCR in PCR reaction tubes for each assay was performed in parallel, with results shown in Table S4. For the NG-positive and CT-positive clinical samples, successful detection of each pathogen was achieved using the UbiNAAT platform. Fluorescence images for an NG-positive clinical sample run showed sample detection in the NG assay pad only (Fig. 5A), with quantified results indicating signal liftoff by 30 minutes (Fig. 5D). Fig. 5B shows that there was



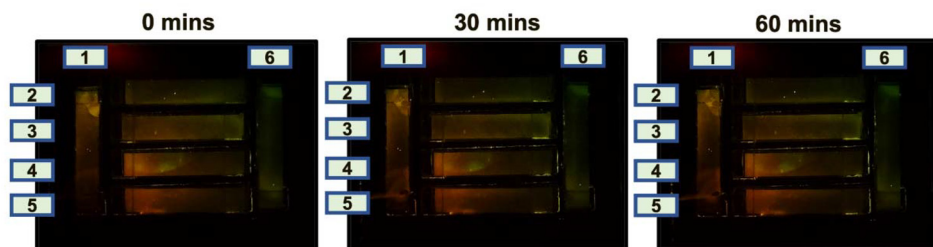
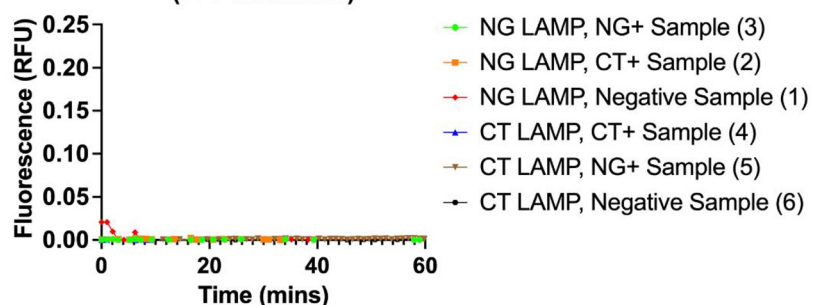
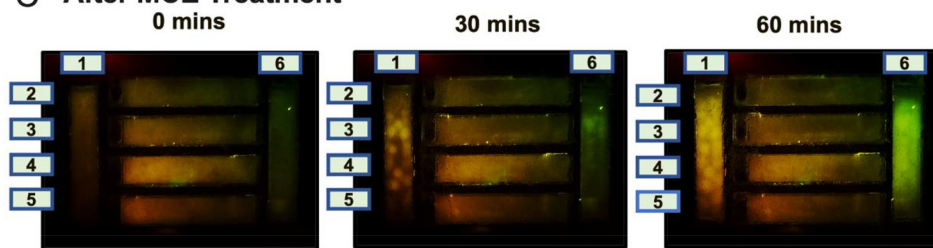
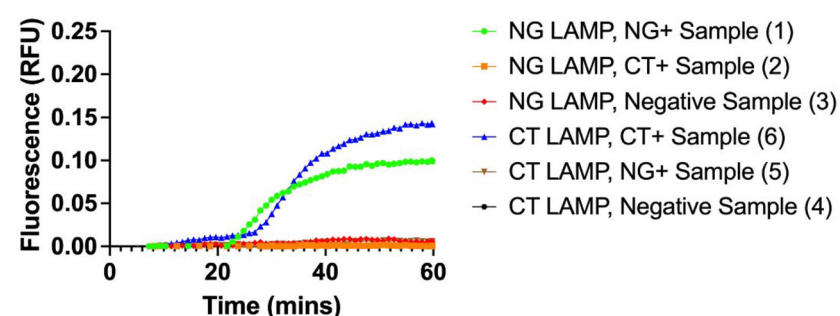
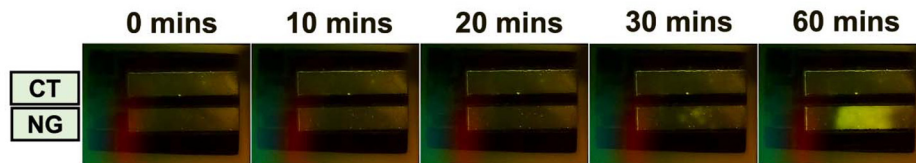
A Before MCE Treatment**B QMA-based LAMP with Clinical Sample (Pre-Treatment)****C After MCE Treatment****D QMA-based LAMP with Clinical Sample (Post-Treatment)**

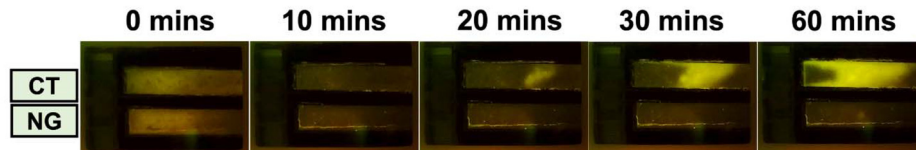
Fig. 4 Filtration of clinical vaginal samples enabled QMA-based LAMP reactions. A non-specific amplification test was included for both *Neisseria gonorrhoeae* (NG) and *Chlamydia trachomatis* (CT) assays. (A) Representative images of the paper-based LAMP reaction with non-treated clinical vaginal samples. The lane number is indicated in parentheses in the legend. (B) Quantified fluorescence curves showed flat signal profiles across positive, negative, and non-specific samples. Results are representative of reproduced replicates (not shown). (C) Representative images of paper-based LAMP reactions with treated clinical vaginal samples. The lane number is indicated in parentheses in the legend. (D) Quantified fluorescence curves show clear positive signals for both NG and CT assays. Cross-reactivity and negative controls showed no fluorescence signal over an hour. Results are representative of reproduced replicates (not shown).



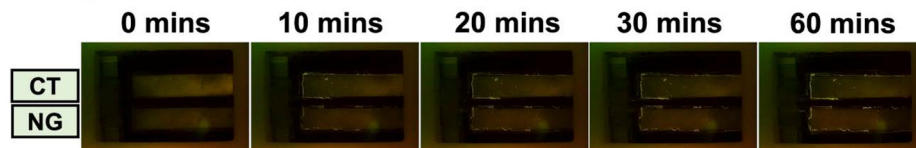
A NG+ Clinical Vaginal Sample on UbiNAAT 2-Plex STI Device



B CT+ Clinical Vaginal Sample on UbiNAAT 2-Plex STI Device

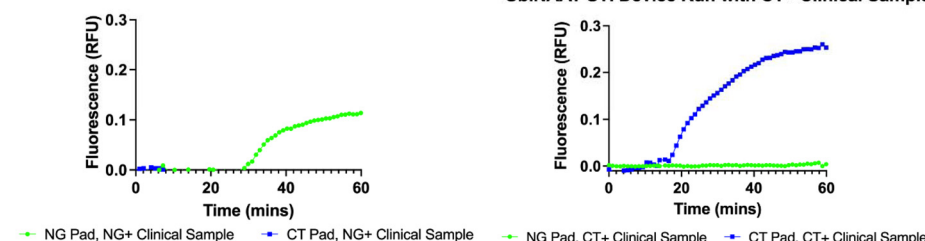


C Negative Clinical Vaginal Sample on UbiNAAT 2-Plex STI Device



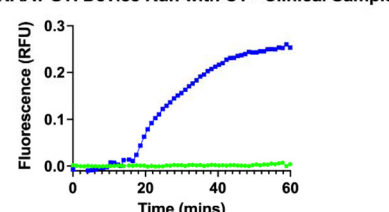
D

UbiNAAT STI Device Run with NG+ Clinical Sample



E

UbiNAAT STI Device Run with CT+ Clinical Sample



F

UbiNAAT STI Device Run with Negative Clinical Sample

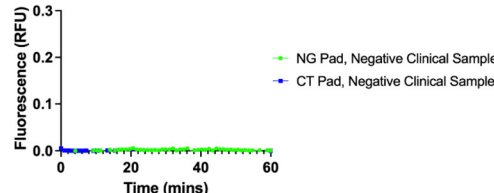


Fig. 5 UbiNAAT 2-plex LAMP detection of *Neisseria gonorrhoeae* (NG) and *Chlamydia trachomatis* (CT) clinical vaginal samples. (A) Real-time LAMP fluorescence signal of NG and CT LAMP with an NG-positive (NG+) sample over an hour. (B) Real-time LAMP fluorescence signal of NG and CT LAMP with a CT-positive (CT+) sample over an hour. (C) Real-time LAMP fluorescence signal of NG and CT LAMP with a negative clinical sample over an hour. (D) Quantified fluorescence curves show a clear NG LAMP signal with the NG+ sample. (E) Quantified fluorescence curves show a clear CT LAMP signal with the CT+ sample. (F) Quantified fluorescence curves show flat signal curves with negative clinical samples.

strong fluorescence amplification across the entirety of the CT assay pad for a CT-positive clinical sample, with the quantified curve indicating signal detection by 20 minutes (Fig. 5E). Neither the NG nor CT-positive samples showed non-specific amplification in the other assay pad, which indicated no contamination. The negative clinical sample showed no detectable fluorescence increase throughout the 60 minutes of amplification (Fig. 5C), with quantified results indicating flat signal curves (Fig. 5F).

Results across the 15 clinical sample runs demonstrated the UbiNAAT's reproducibility and high sensitivity across samples of different bacterial loads, with compiled results showing consistent performance for both assays. All 5 NG-positive samples were successfully detected on the NG LAMP assay pad, with no non-specific amplification in the CT assay pad across each run (Fig. 6A). The lowest observed NG concentration in the clinical samples tested was 3.7×10^3 genome copies per mL, and the highest concentration was 4×10^6

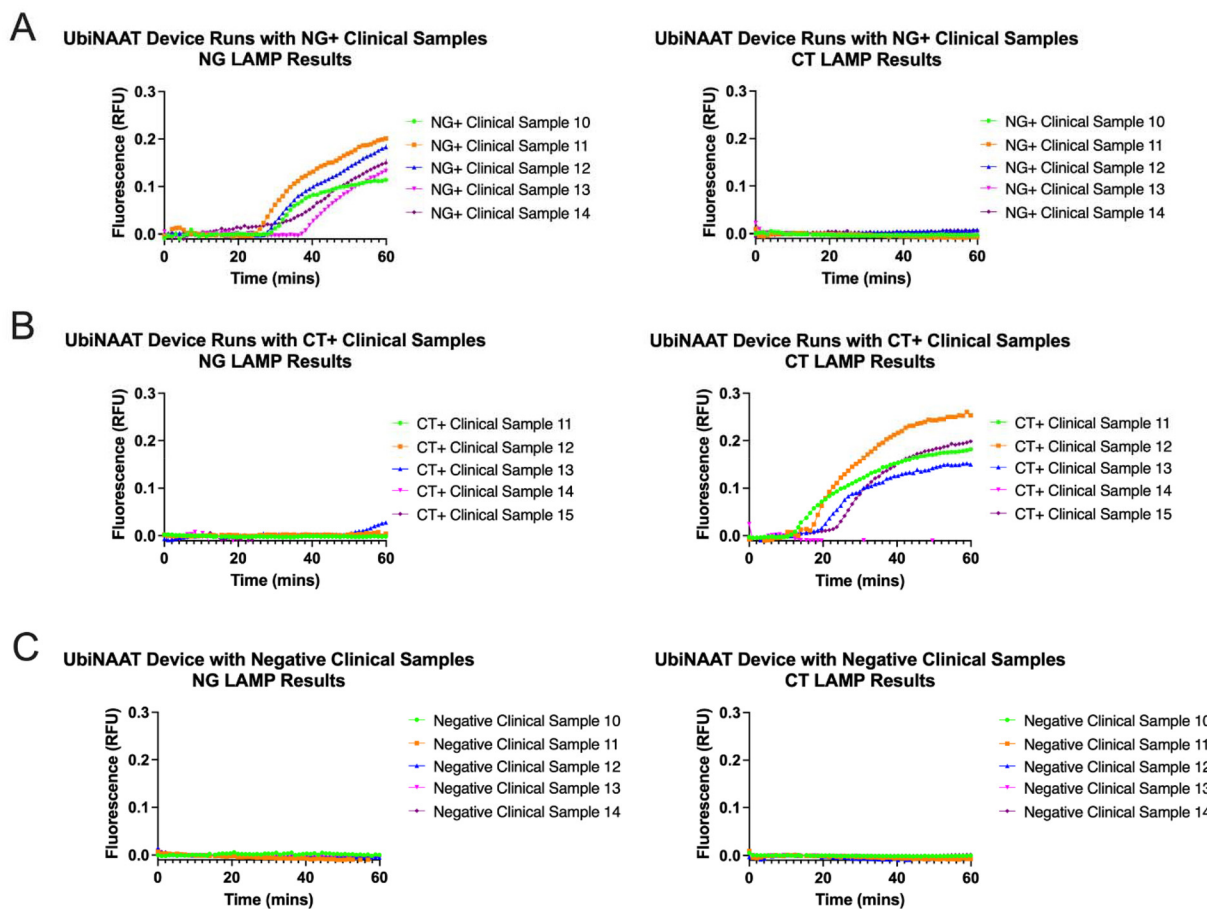


Fig. 6 Compiled results of UbiNAAT assessment of *Neisseria gonorrhoeae* (NG) and *Chlamydia trachomatis* (CT) clinical vaginal samples. (A) UbiNAAT assessment of NG-positive (NG+) clinical vaginal samples across NG LAMP (left) and CT LAMP (right) ($n = 5$). (B) UbiNAAT assessment of CT-positive (CT+) clinical vaginal samples across NG LAMP (left) and CT LAMP (right) ($n = 5$). (C) UbiNAAT assessment of negative clinical vaginal samples across NG LAMP (left) and CT LAMP (right) ($n = 5$).

copies per mL (Table S4). For CT-positive LAMP in the UbiNAAT, 4/5 CT-positive clinical samples showed amplification liftoff prior to 25 minutes, with no non-specific NG assay signal liftoff prior to 55 minutes (Fig. 6B). The range of CT concentrations found in the clinical samples tested was 1.2×10^5 plasmids per mL to 7.1×10^7 plasmids per mL (Table S4). The average clinical sample signal liftoff time for UbiNAAT NG LAMP was 31.8 ± 4.6 minutes across $n = 5$ samples, while CT LAMP showed an average liftoff time of 19.2 ± 4.0 minutes across $n = 4$ samples (Fig. S1). These results indicated that none of the clinical patients were positive for both pathogens, with minimal non-specific activity showing high device specificity. Across $n = 5$ negative clinical samples, neither the NG nor CT LAMP assays showed notable fluorescence amplification across 60 minutes (Fig. 6C). It was noted that 1 of the 5 CT-positive clinical samples resulted in no amplification due to a mechanical failure of the UbiNAAT air spring valve prior to lysis. Despite a high bacterial load in the sample, the lack of a lysis step likely resulted in insufficient recovery of DNA from the patient sample. Subsequent observation of the device did not reveal errors in device assembly. The malfunction may

have been the result of a one-time damaged wax material in the air spring valve.

The 2-plex UbiNAAT assessment of clinical patient samples that were positive for *Neisseria gonorrhoeae* and *Chlamydia trachomatis* infection, combined with previous demonstration of RT-LAMP to detect viral pathogens,³¹ suggests that the platform can be readily adapted for any nucleic acid-based pathogen detection. The performance of each assay for clinical samples of varying bacterial loads indicates compatibility with a sample-to-result time within 60 minutes, with high specificity for each assay and low risk of contamination.

Vaginal infections with CT or NG can lead to significant morbidities, including pelvic inflammatory disease (PID), loss of fertility, and pregnancy complications.^{3,6,15} For these reasons, we focused solely on vaginal swab samples for the first iteration of the STI version of the UbiNAAT diagnostic device. Our success in detecting CT and NG from vaginal swab samples suggests that we may achieve similar success with swab samples from other physiological sites. Previous studies indicate that self-collected swabs from the penile urethral meatus are also a viable alternative to urine or urethral swab



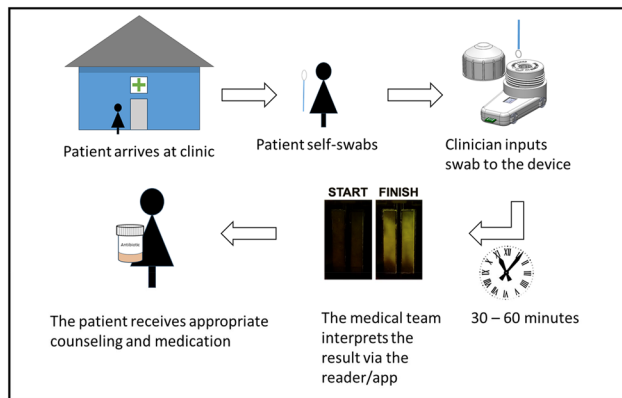


Fig. 7 Proposed future workflow for increased CT/NG screening using the UbiNAAT device in a point-of-care setting.

testing.^{46–48} We hypothesize that our device could accept swabs from the penile urethral meatus without further adaptation, thereby increasing the usefulness of the UbiNAAT for diagnosis of STIs across diverse patient anatomies. NG can also be found in oropharyngeal and anorectal swabs in both men and women.^{48,49} Our previous success with nasal swab samples, coupled with our success here with vaginal swabs, suggests that a similar filtration and deactivation strategy could work for any number of swab samples. Swabs from multiple anatomical sites could be taken from one patient and input to the same low-cost disposable diagnostic UbiNAAT device, maximizing the probability of detecting STIs.

We envision a possible future workflow for this device as shown in Fig. 7. When the patient arrives at the clinic, they will be given a swab and instructions for self-sampling (which can be better tolerated by patients than pelvic exams and clinician-sampling).⁵⁰ The clinician would then take the swab and insert it into the device, where all sample preparation and nucleic acid amplification would occur within 30–60 minutes. The medical team would interpret the results and send the patient home with appropriate treatment. We also envision a use case where initial testing occurs in the home, directed by the patient and using a self-collected swab. The results would be communicated *via* the Internet, an app, or an SMS to a clinician or pharmacist capable of interpreting results and prescribing the appropriate treatment.

Modelling shows that the rapid identification of the correct antimicrobial treatment for each patient could extend the lifetime of previously abandoned first-line antimicrobial drugs against NG.⁵¹ Future work will involve further multiplexing of the device to include NAAT for the identification of antimicrobial resistance markers. We will also incorporate the pre-lysis MCE filtration step into the autonomous device to reduce user steps, improve reproducibility, and make the device ready for use in the clinic or home. Assay sensitivity and operation time could also be improved in future device iterations with the incorporation of a sample concentration step, such as the sequence-specific capture of target DNA.⁵² Once we have a

manufacturable device that can be made on a large scale, we will also expand testing to more strains of NG and CT, as well as samples with known co-infections of these pathogens.

Conclusions

We have shown here a proof of concept for an inexpensive NAAT device for STI detection using clinical vaginal swab samples, with the addition of a filtration step. In this study, all positive and negative NG and CT clinical samples were correctly identified, except for one, which was due to mechanical failure of the device. Our sample-to-result strategy for the low-cost diagnosis of CT and NG from vaginal swab samples demonstrates that this approach is applicable to a wider range of pathogens than those tested in our first publication on the UbiNAAT device. Further multiplexing will increase the diagnostic power of each device, reducing testing costs and increasing access to diagnostic devices globally.

Author contributions

Erin Heiniger and Kevin Jiang: conceived and designed experiments, performed experiments, analysed data, wrote the first draft, and edited and reviewed later drafts; Erin Heiniger: funding acquisition; Sujatha Kumar: conceived and designed experiments, and edited and reviewed later drafts; Paul Yager: conceived and designed experiments, aided in funding acquisition, supervised personnel, and edited and reviewed later drafts.

Conflicts of interest

Paul Yager is both a Professor at UW and a Chief Scientific Officer at UbiDX, which is a small start-up company that has not at this time taken a license to the described technology. There are no further conflicts to declare.

Data availability

Supporting figures and tables can be found at <https://doi.org/10.1039/d5an00496a>. Data supporting this article and its supplementary figures and have been deposited at datadryad.org. See <https://datadryad.org/submission/10.5061/dryad.gf1vhhn26>. Deposited information includes photographs, analysis of the fluorescence intensity from photographs, and qRT-PCR fluorescence data.

Acknowledgements

Research reported in this publication was supported by the United States' National Institute of Biomedical Imaging and Bioengineering of the National Institutes of Health under award number U54EB007958. The content is solely the respons-



sibility of the authors and does not necessarily represent the official views of the National Institutes of Health. Clinical vaginal swab samples were provided by the POCTRN team at Johns Hopkins University. We also acknowledge the generous gift of CT-infected epithelial cells from Laurie Gillette and Richard Burney of Madigan Army Hospital.

References

- 1 World Health Organization (WHO), Global health sector strategies on, respectively, HIV, viral hepatitis and sexually transmitted infections for the period 2022–2030, <https://www.who.int/publications/item/9789240053779>, (accessed 11 June 2024).
- 2 CDC USDH, *Sexually Transmitted Infections Surveillance*, 2022.
- 3 W. Tang, J. Mao, K. T. Li, J. S. Walker, R. Chou, R. Fu, W. Chen, T. Darville, J. Klausner and J. D. Tucker, *Sex. Transm. Infect.*, 2020, **96**, 322–329.
- 4 M. Malekinejad, E. K. Barker, R. Merai, C. M. Lyles, K. T. Bernstein, T. A. Sipe, J. B. Deluca, A. D. Ridpath, T. L. Gift, A. Tailor and J. G. Kahn, *Sex. Transm. Dis.*, 2021, **48**, E138–E148.
- 5 E. C. Ewers, J. M. Curtin and A. Ganesan, *Infect. Dis. Clin. North Am.*, 2023, **37**, 223–243.
- 6 S. S. Cyr, L. Barbee, K. A. Workowski, L. H. Bachmann, C. Pham and K. Schlanger, *Morb. Mortal. Wkly. Rep. Update*, 2020, **69**, 1911–1916.
- 7 S. Hull, S. Kelley and J. L. Clarke, *Popul. Health Manage.*, 2017, **20**, S-1–S-11.
- 8 S. Tuddenham, M. M. Hamill and K. G. Ghanem, *JAMA, J. Am. Med. Assoc.*, 2022, **327**, 161–172.
- 9 E. Jue, N. G. Schoepp, D. Witters and R. F. Ismagilov, *Lab Chip*, 2016, **16**, 1852–1860.
- 10 K. J. Aaron, S. Griner, A. Footman, A. Boutwell and B. Van Der Pol, *Ann. Fam. Med.*, 2023, **21**, 172–179.
- 11 B. J. Masek, N. Arora, N. Quinn, B. Aumakhan, J. Holden, A. Hardick, P. Agreda, M. Barnes and C. A. Gaydos, *J. Clin. Microbiol.*, 2009, **47**, 1663–1667.
- 12 J. Knox, S. N. Tabrizi, P. Miller, K. Petoumenos, M. Law, S. Chen and S. M. Garland, *Sex. Transm. Dis.*, 2002, **29**, 647–654.
- 13 F. Vialard, A. Anand, C. L. Soo, A. De Waal, M. McGuire, S. Carmona, M. Fernández-Suárez, A. A. Zwerling and N. P. Pai, *Sex. Transm. Infect.*, 2023, **99**, 420–428.
- 14 M. Muljadi, C. M. Cheng, C. Y. Yang, T. C. Chang and C. J. Shen, *Front. Bioeng. Biotechnol.*, 2022, **10**, 1–10.
- 15 K. Smolarczyk, B. Mlynarczyk-bonikowska, E. Rudnicka, D. Szukiewicz, B. Meczekalski, R. Smolarczyk and W. Pieta, *MDPI AG*, 2021, preprint, DOI: [10.3390/ijms22042170](https://doi.org/10.3390/ijms22042170).
- 16 M. Rahman, C. Johnson, M. White, J. Ewell, A. Cope, Y. Chandler, T. Bennett, T. Gray, D. Gruber and T. Peterman, *Sex. Transm. Infect.*, 2022, **49**, 257–261.
- 17 E. Welford, T. C. S. Martin, N. K. Martin, W. Tilghman and S. J. Little, *Sex. Transm. Dis.*, 2024, **51**, 388–392.
- 18 S. Huntington, G. Weston and E. Adams, *Ther. Adv. Infect. Dis.*, 2021, **8**, 20499361211061645.
- 19 S. R. Morris, C. C. Bristow, M. R. Wierzbicki, M. Sarno, L. Asbel, A. French, C. A. Gaydos, L. Hazan, L. Mena, P. Madhivanan, S. Philip, S. Schwartz, C. Brown, D. Styers, T. Waymer and J. D. Klausner, *Lancet Infect. Dis.*, 2021, **21**, 668–676.
- 20 Thermo Fisher Scientific, Visby Medical™ Sexual Health Test, <https://www.fishersci.com/shop/products/sexual-health-test/23111204>.
- 21 Y. Zhou, T. T. Jiang, J. Li, Y. P. Yin and X. S. Chen, *EClinicalMedicine*, 2021, **37**, 100961.
- 22 C. A. Cannon, A. K. Piraino, M. R. Golden and L. A. Barbee, *Sex. Transm. Dis.*, 2021, **48**, E168–E170.
- 23 T. Notomi, H. Okayama, H. Masubuchi, T. Yonekawa, K. Watanabe, N. Amino and T. Hase, *Nucleic Acids Res.*, 2000, **28**(12), E63.
- 24 K. Nagamine, T. Hase and T. Notomi, *Mol. Cell. Probes*, 2002, **16**, 223–229.
- 25 P. Francois, M. Tangomo, J. Hibbs, E. J. Bonetti, C. C. Boehme, T. Notomi, M. D. Perkins and J. Schrenzel, *FEMS Immunol. Med. Microbiol.*, 2011, **62**, 41–48.
- 26 M. Parida, G. Posadas, S. Inoue, F. Hasebe and K. Morita, *J. Clin. Microbiol.*, 2004, **42**, 257–263.
- 27 S. Sen, P. Bhowmik, S. Tiwari, Y. Peleg and B. Bandyopadhyay, *Mol. Biol. Rep.*, 2024, **51**(1), 211.
- 28 M. Mostafa, A. Barhoum, E. Sehit, H. Gewaid, E. Mostafa, M. M. Omran, M. S. Abdalla, F. M. Abdel-Haleem, Z. Altintas and R. J. Forster, 2022, preprint, DOI: [10.1016/j.trac.2022.116750](https://doi.org/10.1016/j.trac.2022.116750).
- 29 L. T. N. Ngoc and Y. C. Lee, *Biosensors*, 2024, **14**(2), 97.
- 30 Y. Wang, J. Chen, Z. Yang, X. Wang, Y. Zhang, M. Chen, Z. Ming, K. Zhang, D. Zhang and L. Zheng, 2024, preprint, DOI: [10.3390/molecules29112417](https://doi.org/10.3390/molecules29112417).
- 31 K. P. Jiang, S. Bennett, E. K. Heiniger, S. Kumar and P. Yager, *Lab Chip*, 2024, **24**, 492–504.
- 32 S. O. Hjelmevoll, M. E. Olsen, J. U. E. Sollid, H. Haaheim, M. Unemo and V. Skogen, *J. Mol. Diagn.*, 2006, **8**, 574–581.
- 33 B. Dhawan, J. Rawre, A. Ghosh, N. Malhotra, M. M. Ahmed, V. Sreenivas and R. Chaudhry, *Indian J. Med. Res.*, 2014, **140**, 252–261.
- 34 C. Myhrvold, C. A. Freije, J. S. Gootenberg, O. O. Abudayyeh, H. C. Metsky, A. F. Durbin, M. J. Kellner, A. L. Tan, L. M. Paul, L. A. Parham, K. F. Garcia, K. G. Barnes, B. Chak, A. Mondini, M. L. Nogueira, S. Isern, S. F. Michael, I. Lorenzana, N. L. Yozwiak, B. L. MacInnis, I. Bosch, L. Gehrke, F. Zhang and P. C. Sabeti, *Science*, 2018, **360**, 444–448.
- 35 B. A. Rabe and C. Cepko, *Proc. Natl. Acad. Sci. U. S. A.*, 2020, **117**, 24450–24458.
- 36 S. Kumar, R. Gallagher, J. Bishop, E. Kline, J. Buser, L. Lafleur, K. Shah, B. Lutz and P. Yager, *Analyst*, 2020, **145**, 6875–6886.
- 37 K. G. Shah, S. Kumar and P. Yager, *Sci. Rep.*, 2022, **12**(1), 14618.



38 K. G. Shah, M. Roller, S. Kumar, S. Bennett, E. Heiniger, K. Looney, J. Buser, J. D. Bishop and P. Yager, *PLoS One*, 2023, **18**, 1–16.

39 K. G. Shah, S. Kumar, V. Singh, L. Hansen, E. Heiniger, J. D. Bishop, B. Lutz and P. Yager, *Anal. Chem.*, 2020, **92**, 13066–13072.

40 K. G. Shah, V. Singh, P. C. Kauffman, K. Abe and P. Yager, *Anal. Chem.*, 2018, **90**, 6967–6974.

41 M. L. Liu, Y. Xia, X. Z. Wu, J. Q. Huang and X. G. Guo, *AMB Express*, 2017, **7**(1), 48.

42 Q. Zhou, R. Yu, D. Xia, J. Liu, W. Xu and Y. Yin, *Indian J. Microbiol.*, 2022, **62**, 428–433.

43 M. Goto, E. Honda, A. Ogura, A. Nomoto and K. I. Hanaki, *BioTechniques*, 2009, **46**, 167–172.

44 A. Ito and K. Ueno, *Bunseki Kagaku*, 1970, **19**, 393–397.

45 M. B. Sørensen, I. A. Bergdahl, N. H. I. Hjøllum, J. P. E. Bonde, M. Stoltenberg and E. Ernst, *Mol. Hum. Reprod.*, 1999, **5**, 331–337.

46 L. Dize, P. Barnes, M. Barnes, Y. H. Hsieh, V. Marsiglia, D. Duncan, J. Hardick and C. A. Gaydos, *Diagn. Microbiol. Infect. Dis.*, 2016, **86**, 131–135.

47 J. H. Melendez, A. Muñiz Tirado, A. Onzia, E. Mande, J. P. Hardick, R. Parkes-Ratanshi, M. M. Hamill and Y. C. Manabe, *Sex. Transm. Infect.*, 2025, **101**(4), 247.

48 L. Berry and B. Stanley, *J. Med. Microbiol.*, 2017, **66**, 134–136.

49 B. M. J. W. Van Der Veer, C. J. P. A. Hoebe, N. H. T. M. Dukers-Muijres, L. B. Van Alphen and P. F. G. Wolffs, *J. Clin. Microbiol.*, 2020, **58**(11), e001171.

50 M. Muljadi, C.-M. Cheng, C.-Y. Yang, T.-C. Chang and C.-J. Shen, *Front. Bioeng. Biotechnol.*, 2022, **10**, 1–10.

51 K. M. Turner, H. Christensen, E. J. Adams, D. McAdams, H. Fifer, A. McDonnell and N. Woodford, *BMJ Open*, 2017, **7**, 1–9.

52 A. Oreskovic, N. Panpradist, D. Marangu, M. Ngwane, Z. Magcaba, S. Ngcobo, Z. Ngcobo, D. Horne, D. Wilson, A. Shapiro, P. Drain and B. Lutz, *J. Clin. Microbiol.*, 2021, **59**, e0007421.

